Available online at www.sciencedirect.com
ScienceDirect
International Journal of Mechanical Sciences 50 (2008) 752–763
International Journal of MECHANICAL SCIENCES
www.elsevier.com/locate/ijmecsci

Non-smooth modelling of billiard- and superbilliard-ball collisions

Antonio Doménech

Department of Analytical Chemistry, University of Valencia, Dr. Moliner, 50, 46100 Burjassot (València), Spain

Received 11 June 2007; received in revised form 9 November 2007; accepted 18 November 2007
Available online 22 November 2007

Abstract

A description of billiard-ball collisions using a 'discontinuous' model is presented considering a two-step situation corresponding to the ball–ball interaction followed by ball-supporting surface interaction. It is applied to the inelastic impact of a cue ball having arbitrary pivotment and 'English' spins against an object ball initially at rest. This formulation provides a simplified approximation to the 'continuous' models of impact and considers two different regimes of impact: gross slip, and slip–stick, described in terms of coefficients of friction and restitution. As a result, the angles of scattering of the balls just after the impact (post-collision angles) and when the ball reach pure rolling motion (post-transition angles) are expressed in terms of the angle of impact, the mass ratio, and the initial spin conditions. Theoretical predictions are compared with experimental data for different materials, including regulation billiard ball and superballs.

Keywords: Billiards; Impact; Non-smooth mechanics; Friction; Restitution

1. Introduction

From the seminal work of Coriolis [1], billiard-ball collisions have claimed considerable attention along time. In general, the impact event is described in terms of a discontinuous change in the velocities of the balls where the collision is treated as inelastic and frictionless [2]. This type of descriptions falls within the so-called non-smooth dynamics, where collisions are described in terms of 'instantaneous' forces acting on a single contact point.

In the context of such discontinuous or non-smooth mechanics, billiard-ball collisions can be described within the more general formulation of impact due to Brach [3] and Kane and Levinson [4]. These authors consider friction effects during the 'instantaneous' impact event, so that two impact regimes, with and without sliding between the contacting points of the colliding bodies, are predicted. The inelasticity of the impact is described in terms of the coefficient of restitution, e, the condition of no sliding being formulated by equalizing tangential velocities of the contacting points of the bodies at the end of the impact. When sliding exists through the impact, tangential forces are taken as frictional forces using the Amontons–Coulomb law by introducing the coefficient of friction, μ. Alternatively, tangential coefficients of restitution [5], and moment coefficient of restitution [3] can be defined. In the more recent formulation of Chatterjee and Ruina [6], the normal impulse is taken as an independent variable so that terminal tangential to normal impulse ratio characterizes the impact. For collisions with continuous sliding in any direction, this ratio equals the coefficient of friction.

Alternatively, collisions can be described in terms of continuous forces acting along a finite time between the contacting points of the colliding objects, as taken by Keller for impact with sliding between rigid bodies [7]. Here, mechanical properties of bodies during collision can be represented in different ways. Thus, Maw et al. [8,9] obtained an inelasticity solution for the traction distribution in annuli surrounding the contact point for the collinear impact between rough spheres subjected to both tangential and normal relative displacement. Alternatively, the small deforming region of contact can be represented as a deformable massless particle. The compliance of a small elastoplastic region around the contact point of one body is then represented by discrete elements, oriented in the normal and tangential directions, connected to the massless

E-mail address: antonio.domenech@uv.es

0020-7403/$ - see front matter © 2007 Elsevier Ltd. All rights reserved.
doi:10.1016/j.ijmecsci.2007.11.006

particle which can either stick or slide on the surface of the second body, as described by Stronge [10–13]. By employing specific compliance relations one obtains smooth dynamics of the time-dependent processes of stick and/or sliding occurring during the impact, depending on the relative tangential velocity of the contacting points of bodies.

Following the recent formulation of Stronge et al. [12,13], if the tangential relative velocity is sufficiently large, there is continuous slip in the initial direction throughout the contact period. In this case gross slip occurs so that the velocity of slip only slows during impact. If the initial tangential relative velocity is small, so that the ratio of tangential to normal force is less than the coefficient of friction, μ, the contact initially sticks until a terminal period of slip is attained. Finally, for intermediate tangential relative velocity, there is initial slip at the contacting point until the speed of slip has slowed sufficiently so that stick can occur. In the following period of stick, the tangential relative velocity is reduced until the direction of the tangential force reverses. This intermediate period of stick persists until the reversed tangential force is as large as the friction limit and then sliding is re-established. Accordingly, for planar collisions with friction, three impact regimes can be distinguished: stick–slip, slip–stick–slip, and gross slip or continuous slip. Experimental data using microforce sensing in various configurations [14–18], have confirmed general trends of such continuous models, tangential force reversal and different impact regimes, in particular.

The case of the impact between billiard balls is complicated because not only a ball–ball interaction, but also a sphere-supporting surface interaction, has to be accounted. Here, friction effects play a crucial role with regard of post-collision paths of the balls. In fact, frictionless models are unable to explain the paths of the balls when 'English' spin effects (forward/topspin and backward/backspin, pivoting spin) are imparted to the balls [19]. The incorporation of surface friction into theory of particle collision is of interest in a wide variety of applications; in particular, for modelling the dynamics of granular matter [20,21].

Remarkably, predictions from discontinuous and continuous models coincide when slip exists throughout the impact [10–13], so that differences are concentrated in the no-sliding collision regime. Additionally, it should be emphasized that, with regard to post-collision velocity, stick–slip and slip–stick–slip and gross slip regimes can be reduced solely to a stick and a gross slip responses.

It is reported here a single, 'discontinuous' model for the impact between rigid spheres moving on a rough, infinitely massive, horizontal surface that incorporates the essential features resulting from the continuous model of Stronge [10–13] into a discontinuous frame for the general case in which the cue ball has arbitrary values of English spins. As a result, a series of velocity-independent equations relating the post-collision and post-transition angles defined by the balls after the impact, with the angle of impact, the mass ratio and the coefficients of restitution and friction, are obtained. This formulation incorporates, following Marlow [22] and Alciatore [23], friction with the pool and extends prior studies on billiard-ball collisions [24], and ball rebounds on horizontal rough surfaces [25] where a discontinuous model based on the formulations of Brach, and Kane and Levinson was discussed. In agreement with literature [2–25], the coefficients of restitution and friction will be taken here as material-dependent, velocity-independent constants. Experimental data on steel, rubber, and regulation billiard balls are used in addition to some literature data for testing the proposed relationships.

2. Theory

2.1. General approach

Let us consider the collision between two homogeneous spheres moving on a flat horizontal surface. As schematized in Fig. 1, a normal-tangential coordinate system is chosen such that the line through the sphere centres is the normal axis (x). The tangential axis (y) is perpendicular to the normal axis and lies in a horizontal plane parallel to the supporting surface. The z-axis is defined by the outward direction normal from the supporting surface. It is assumed that the cue sphere 1 is projected with a linear velocity v_o against the object sphere 2 which is initially at rest. We consider the case in which a forward horizontal spin, ω_o, with components ω_{ox}, ω_{oy}, along the x, y, axes, and a vertical (or pivotment) spin, ω_{oz}, along the z-axis are imparted to the cue sphere.

In conventional 'discontinuous' rigid body mechanics the impact event is represented in terms of 'instantaneous' normal and tangential impulses, F_n, F_t, which can be

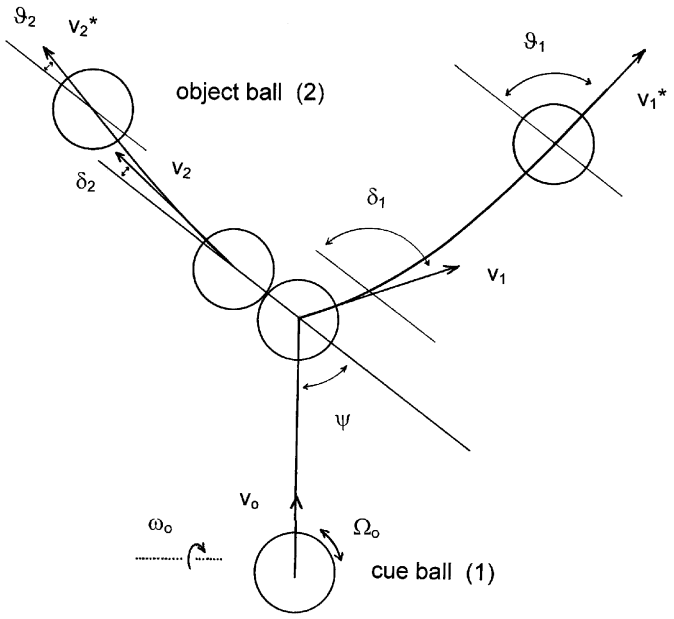

Fig. 1. Schematics for the impact between billiard balls.

expressed in terms of the changes in momentum. Considering separately the horizontal and vertical components of the tangential impulse, F_{th}, F_{tv}, one can write:

$$F_n = -m_1(v_{1x} - v_{ox}) = m_2 v_{2x}, \tag{1}$$

$$F_{th} = -m_1(v_{1y} - v_{oy}) = m_2 v_{2x}, \tag{2}$$

where v_{ox}, v_{oy} represent the components of the centre of mass velocity of the cue sphere before the impact, and v_{jx}, v_{jy} $(j = 1, 2)$ the components for the centre of mass velocity of both spheres immediately after the collision.

For a collinear collision, the normal and tangential impulsive forces can be treated as independent. The spheres modify their angular velocities by effect of the torque imparted by the tangential forces during the impact. Taking initial angular velocity components $\omega_{2x}(0) = 0$, $\omega_{2y}(0) = 0$, $\omega_{ox} = \omega_o \sin\psi$, $\omega_{oy} = \omega_o \cos\psi$, the corresponding values after the impact will be, $\omega_{2x} = 0$, $\omega_{1x} = \omega_{ox} = \omega_o \sin\psi$, and

$$RF_{tv} = -I_1(\omega_{1y} - \omega_{oy}) = I_2\omega_{2y}, \tag{3}$$

$$RF_{th} = I_1(\omega_{z1} - \omega_{zo}) = -I_2\omega_{z2}. \tag{4}$$

Notice that this formulation can easily be applied to billiard-ball collisions taking $M = 1$, and to describe the rebound of a sphere against a rough, infinitely massive vertical plane taking $M = 0$.

Introducing the angles of impact and scattering depicted in Fig. 1 and taking $M = m_1/m_2$, Eqs. (1) and (2) can be rewritten as

$$M(v_o \cos\psi - v_1 \cos\delta_1) = v_2 \cos\delta_2, \tag{5}$$

$$M(v_o \sin\psi - v_1 \sin\delta_1) = v_2 \sin\delta_2. \tag{6}$$

The inelasticity of the impact can be described, as usually, in terms of the 'normal' coefficient of restitution, e, defined as the negative ratio between the normal components of the relative velocity of the points of contact after and before the impact.

In the studied case this definition yields

$$e = (v_2 \cos\delta_2 - v_1 \cos\delta_1)/v_o \cos\psi. \tag{7}$$

Accordingly, the normal impulse can be expressed as

$$F_n = m_1\left(\frac{1+e}{1+M}\right)v_o \cos\psi. \tag{8}$$

In this formulation, there is a vertical frictional contact impulse at the nominal contact between spheres, due to forward spin. Here, it is considered the case in which the cue sphere is launched with a forward spin, so that the vertical impulse acts downwards on the sphere 2, and upwards to the sphere 1. Accordingly, the sphere 1 jumps off the horizontal surface. As far as this effect does not affect significantly the horizontal components of velocity, the separation of the sphere 1 from the pool will be ignored in the following.

In this scheme, the sphere 2 is submitted to impulsive forces resulting from its interaction with the horizontal surface. As schematized in Fig. 2, these forces can be described in terms of a main normal reaction impulse, N, and a frictional impulse, F_f, subsequently decomposed into its components in the x and y directions, F_{fx}, F_{fy}. Here N can be taken as equal to F_{tv}, a condition that ensures that the vertical component of the centre of mass velocity of the sphere 2 is strictly equal to zero after the impact. Assuming that $F_{tv} \neq 0$, so that the linear and angular velocities of the sphere 2 immediately after the impact will be given by

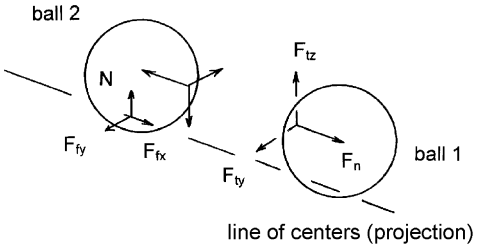

Fig. 2. Impulse 'free-body' diagram for a cue ball with forward 'English' spin striking a object ball initially at rest.

$$m_2 v_{2x} = v_2 \cos\delta_2 = F_n + F_{fx}, \tag{9}$$

$$m_2 v_{2y} = v_2 \sin\delta_2 = F_{ty} - F_{fy}, \tag{10}$$

$$m_2 R\omega_{2x} = (5/2)F_{fy}, \tag{11}$$

$$m_2 R\omega_{2y} = (5/2)(F_{tv} - F_{fx}). \tag{12}$$

These equations apply at termination of impact if $F_{tv} \neq 0$. For the spin about vertical axis one can write

$$m_2 R\omega_{z2} = -m_1(R\omega_{z1} - R\omega_{zo}) = (5/2)F_{th}. \tag{13}$$

As a result of the impact, the spheres are projected along the horizontal plane with a combination of translation and rotation motions. Then, friction with the horizontal surface determines, as described by Hopkins and Patterson [26], that the spheres describe curved paths until the pure rolling motion is finally established. This situation corresponds to rectilinear motions defining post-transition angles, ϑ_1, ϑ_2, as shown in Fig. 1. The law of angular momentum yields, for the centre of mass velocities when pure rolling motion is reached, $v^*_{jx} = R\omega^*_{jy}$, $v^*_{jy} = R\omega^*_{jx}$ $(j = 1, 2)$: $Rm_j(v^*_{jx} - v_{jx}) = -I_j(\omega^*_{jy} - \omega_{jy})$ and $Rm_j(v^*_{jyx} - v_{jy}) = -I_j(\omega^*_{jx} - \omega_{jx})$, so that

$$v^*_{jx} = (5/7)v_{jx} + (2/7)R\omega_{jy}, \tag{14}$$

$$v^*_{jy} = (5/7)v_{jy} + (2/7)R\omega_{jx}. \tag{15}$$

Combining the above equations, one can obtain velocity-independent equations for post-collision and post-transition angles in function of the angle of impact, the mass ratio, M, and the coefficients of restitution and friction (*vide infra*) providing that appropriate force laws are used. In the following we consider different 'discontinuous' cases derived from the 'continuous' formulation of Stronge [10–13].

2.2. Gross slip case

We consider that sliding exists in the contact between spheres 1 and 2 and between the sphere 2 and the supporting horizontal surface. Assuming that Amontons–Coulomb friction is operative, the conditions $F_t = \mu F_n$, and $F_f = \mu' N$ hold, μ and μ' being, respectively, the coefficients of (kinetic) sliding friction between spheres 1 and 2 and between the sphere 2 and the supporting surface. To estimate the horizontal and vertical components of the tangential force, it is assumed in the following that the direction of the tangential force is that of the relative velocity of the contacting points of the spheres at the beginning of the impact. Introducing the angle σ, defined by the directions of the horizontal component of the tangential velocity at the point of contact just after the impact and its component along the y-axis, the above condition yields

$$\tan\sigma = \frac{v_o \sin\psi + R\Omega_o}{R\omega_o \cos\psi} = \frac{F_{th}}{F_{tv}}. \tag{16}$$

To propose a similar relation for the components of F_f, we introduce the velocities of the point of contact of the sphere 2 with the supporting surface resulting from the sole action of the F_n and F_t impulses. Now, one introduces the angle φ between the velocity of the sphere 2-pool contact just after the impact and its component along the y-axis. Then,

$$\tan\varphi = \frac{F_{th}}{F_n + (5/2)F_{tv}} = \frac{F_{fy}}{F_{fx}}. \tag{17}$$

In this scheme,

$$F_{th} = \mu F_n \sin\sigma = \mu m_1 \left(\frac{1+e}{1+M}\right) v_o \cos\psi \sin\sigma, \tag{18}$$

$$F_{tv} = \mu F_n \cos\sigma = \mu m_1 \left(\frac{1+e}{1+M}\right) v_o \cos\psi \cos\sigma, \tag{19}$$

$$F_{fy} = \mu' N \sin\varphi = \mu'\mu m_1 \left(\frac{1+e}{1+M}\right) v_o \cos\psi \cos\sigma \sin\varphi, \tag{20}$$

$$F_{fx} = \mu' N \cos\varphi = \mu'\mu m_1 \left(\frac{1+e}{1+M}\right) v_o \cos\psi \cos\sigma \cos\varphi. \tag{21}$$

Combining Eqs. (16)–(21) with Eqs. (5)–(7), one can arrive to the following velocity-independent equations for the scattering angles

$$\tan\delta_1 = \left(\frac{1+M}{M-e}\right)\tan\psi - \mu\left(\frac{1+e}{M-e}\right)\sin\sigma, \tag{22}$$

$$\tan\delta_2 = \frac{\mu(\sin\sigma - \mu'\cos\sigma\sin\varphi)}{1 - \mu\mu'\cos\sigma\cos\varphi}, \tag{23}$$

Where $\tan\varphi = \mu\sin\sigma/[1 + (5/2)\,\mu\cos\sigma]$. Using Eqs. (14) and 15, one can arrive to the following expressions for the post-transition angles:

$$\tan\vartheta_1 = \frac{(1+M)(5/2 + R\omega_o/v_o)\tan\psi - (5/2)\mu(1+e)\sin\sigma}{(1+M)(R\omega_o/v_o) + (5/2)(M-e) - (5/2)\mu(1+e)\cos\sigma}, \tag{24}$$

$$\tan\vartheta_2 = \frac{\mu\sin\sigma}{1 - \mu\cos}. \tag{25}$$

This formulation contains a previous formulation [24] taking $\mu' = 0$, and reduces to that of Wallace and Schroeder [2] by inserting $M = 1$, $e = 1$, $\mu = 0$, $\mu' = 0$.

2.3. Discontinuous description of impact with stick–slip

Following Brach [3] and Kane and Levinson [4], under determined conditions sliding motion ceases during the impact event so that the tangential components of the velocities of the contacting points of the spheres equal to zero just after the collision. Here, Eqs. (18)–(21) are not valid and a new set of impulse functions has to be calculated. The no-slip condition at impact point can be expressed by means of the relationships:

$$v_2 \sin\delta_2 + R\omega_{z2} = v_1 \sin\delta_1 - R\omega_{z1}, \tag{26}$$

$$v_{2z} - R\omega_{1y} = v_{1z} + R\omega_{2y}. \tag{27}$$

Accordingly, the horizontal and vertical components of the tangential impulse becomes

$$F_{th} = \frac{(2/7)m_1}{(1+M)}(v_o \sin\psi + R\omega_{zo}), \tag{28}$$

$$F_{tv} = \frac{(2/7)m_1}{(1+M)} R\omega_o \cos\psi. \tag{29}$$

Remarkably, these components satisfy Eq. (16).

Following Stronge [10–13], the situation is more complicated, because for low relative tangential velocities, stick–slip, and slip–stick–slip regimes of impact can take place. Both regimes can be unified, however, within a unique slip–stick behaviour following the approaches of Walton [27] and Foerster et al. [28].

To translate the above no-sliding regimes into a non-smooth formulation, one can take an operational approach whose discussion will be presented for the rebound of a homogeneous sphere on a rough horizontal surface. This situation has been treated by several authors using discontinuous [17,18,24,29] and continuous [10–14] models. Let us consider a homogeneous sphere impacting obliquely a horizontal plane with velocity v_o and no spin. The normal impulse is given by $F_y = -mv_{oy}(1+e)$, so that the vertical component of the centre of mass velocity just after the impact is $v_y = -ev_{oy}$. The horizontal component centre of mass velocity and the angular velocity of the sphere just after the impact are given by $v_x = v_{ox} - F_x/m$ and $R\omega = (5/2)(F_x/m)$, while the tangential velocity of the contacting point at the separation, V_x, is equal to $v_x + R\omega$.

In the case of continuous slip, the horizontal impulse, F_x, is given by

$$F_x = \mu F_y = -\mu(1+e)mv_{oy}. \tag{30}$$

Here the post-collision horizontal component centre of mass velocity and the angular velocities are $v_x = v_{ox} - \mu(1+e)v_{oy}$ and $R\omega = -(5/2)\mu(1+e)v_{oy}$, whereas the velocity of the contacting point immediately after the impact is given by $V_x = v_{ox} - (7/2)\mu(1+e)v_{oy}$. Accordingly, predicted plots of $V_x/\mu v_{oy}$ vs. $v_{ox}/\mu v_{oy}$, used by Maw et al. [8,9] and Stronge [10], consist of a straight line of slope 1 and ordinate at the origin $-(7/2)(1+e)$.

In the classical discontinuous formulation of no-slip impact [3,4], the velocity of the contacting point at the separation becomes zero and then

$$F_x = -(2/7)mv_{ox}. \tag{31}$$

To provide a non-smooth formulation of slip–stick, one can consider a simplified representation in which the sphere produces a small deformation in the supporting surface as described by Hutchings et al. [29] for the impact of hard spheres against a ductile, infinite plane. In smooth mechanics, the small deforming region of contact of the sphere is represented by discrete tangential and normal compliance elements connected to a massless particle which stick on the surface of the second body. To provide a non-smooth model for that situation, it will be assumed that during the 'instantaneous' impact event, the rough horizontal plane is deformed so that the sphere sticks and slips along a small spherical-shaped deformed surface, so that the horizontal impulse, F_x, is accompanied by a friction impulse, F_s, as illustrated in Fig. 3. This friction impulse should contribute to both the total horizontal and vertical impulses acting on the sphere. Obviously, representation in Fig. 3 overestimates the size of the deformed region. This representation must be viewed as an 'equivalent system', as compliance formalism used in smooth impact mechanics, rather than a realistic description of the sphere deformation occurring in the impact event [30].

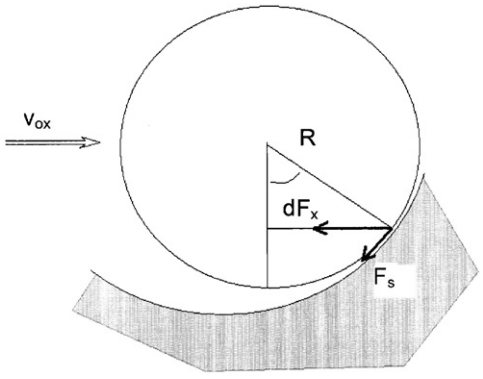

Fig. 3. Non-smooth modelling of the impact of a rigid sphere against a deformable horizontal plane. Schematics in the plane of the initial velocity of the sphere where the deformation is highly overestimated.

It will be used an operational approach, similar to Walton's treatment [27], assuming that: (i) F_s contributes to the horizontal impulse so that the total horizontal impulse acting on the sphere equals to that described by the classical discontinuous model [3,4]; (ii) the contribution of F_s to the vertical impulse is negligible; (iii) F_s creates an additional torque of magnitude $-(2/7)\mu RF_x$. Accordingly, one can write

$$m(v_x - v_{ox}) = -(2/7)mv_{ox}, \tag{32}$$

$$R\omega = -(5/2)(2/7)[1+(2/7)\mu]v_{ox}. \tag{33}$$

As a result, the velocity of the point of contact of the sphere at the end of the impact will satisfy the relationship:

$$V_x = -(10/49)\mu v_{ox}. \tag{34}$$

Then, plots of $V_x/\mu v_{oy}$ vs. $v_{ox}/\mu v_{oy}$, yield a straight line of slope $-10/49$ and y-intercept close to zero.

To describe impact event in slip–stick regime in two-sphere collisions, a simplified approach will be taken. It will be assumed that the net normal and tangential impulses are equal to those given by the conventional discontinuous model whereas a total torque of magnitude $-(2/7)[1+(2/7)\mu]RF_t$ appears.

In the following three possible cases will be considered, involving slip–stick (denoted by s) and/or sliding (denoted by μ) in the sphere–sphere and sphere 2-horizontal supporting surface interactions. These will be represented, by simplicity, as s–μ, μ–s, and s–s. This scheme is completed by the case in which sliding exists in both interactions ($\mu-\mu$ case), discussed in the previous section.

2.4. s–μ case

It is considered here that sliding exists during the impulsive interaction between the sphere 2 and the horizontal surface. This situation will be described using Eqs. (8), (28) and (29) so that post-collision angle δ_1 becomes

$$\tan\delta_1 = \left(\frac{M+5/7}{M-e}\right)\tan\psi - \left(\frac{2/7}{M-e}\right)\frac{R\omega_{zo}}{v_o\cos\psi}. \tag{35}$$

Now, a torque τ_y equal to $-(2/7)RF_{tv}(1+(2/7)\mu\cos\sigma)$ appears so that Eq. (17) is replaced by

$$\tan\varphi = \frac{(2/7)(v_o\sin\psi + R\omega_{zo})}{(1+e)v_o\cos\psi + (5/7)(1+(2/7)\mu\cos\sigma)R\omega_o\cos\psi}. \tag{36}$$

The forces acting on the sphere 2 by effect of its interaction with the supporting surface will be

$$F_{fx} = \frac{(2/7)\mu' m_1 R\omega_o\cos\psi\cos\varphi}{1+M}, \tag{37}$$

$$F_{fy} = \frac{(2/7)\mu' m_1 R\omega_o\cos\psi\sin\varphi}{1+M}. \tag{38}$$

Combining Eqs. (36)–(38), with Eqs. (5)–(12), one obtains for the post-collision angle δ_2:

$$\tan\delta_2 = \frac{\tan\psi + R\Omega_o/v_o\cos\psi - \mu'(R\omega_o/v_o)\sin\varphi}{(7/2)(1+e) - [(2/7)\mu\cos\sigma + \mu'\cos\varphi](R\omega_o/v_o)}. \quad (39)$$

The corresponding equations for post-transition angles ϑ_1, ϑ_2, can be derived from the above and Eqs. (14), (15), resulting the expressions:

$$\tan\vartheta_1 = \frac{[(M+5/7)+(2/5)(R\omega_o/v_o)]\tan\psi - (2/7)(R\omega_{zo}/v_o\cos\psi)}{M - e + [(2/5)(1+M) - (2/7)[1+(2/7)\mu\cos\sigma](R\omega_o/v_o)}, \quad (40)$$

$$\tan\vartheta_2 = \frac{\tan\psi + R\omega_{zo}/v_o\cos\psi}{(7/2)(1+e) - [1+(2/7)\mu](R\omega_o/v_o)}. \quad (41)$$

It should be noted that the slip contribution of the slip–stick regime (given by μ-containing terms) in the sphere 1–sphere 2 contact appears for post-transition angles but not for post-collision ones. Remarkably, the effect of sliding in the sphere 2-horizontal surface interaction, expressed by μ'-containing terms, cancels for ϑ_2, only remaining for δ_2.

2.5. s–s case

In this case, it is assumed that slip–stick conditions are valid in both the sphere–sphere interaction and the sphere 2-supporting surface interaction. Accordingly, Eqs. (28), (29) are again used so that post-collision angle δ_1 and post-transition angle ϑ_1 are again described by Eqs. (35) and (40), respectively. For obtaining angles δ_2 and ϑ_2, it is assumed that the tangential velocity of the contacting point of the sphere 2 with the horizontal surface equals to zero just after the overall impact event. This assumption leads to

$$F_{fy} = \frac{(2/7)(2/7)m_1(v_o\sin\psi + R\omega_{zo})}{1+M}, \quad (42)$$

$$F_{fx} = \frac{(2/7)m_1[(1+e)v_o\cos\psi + (5/7)(1+(2/7)\mu\cos\varphi)R\omega_o\cos\psi}{1+M}. \quad (43)$$

Using Eqs. (42), (43) conjointly with Eqs. (12)–(15), one can arrive at

$$\tan\delta_2 = \frac{\tan\psi + R\omega_{zo}/v_o\cos\psi}{(7/2)(1+e) - [1+(2/7)\mu\cos\sigma](R\omega_o/v_o)}. \quad (44)$$

Now, considering the conditions imposed by Eqs. (14) and 15, the post-transition angle ϑ_2 becomes

$$\tan\vartheta_2 = \frac{[1+(2/7)\mu'\sin\varphi](\tan\psi + R\omega_{zo}/v_o\cos\psi)}{(1+e)[7/2+(2/7)\mu'\cos\varphi] - [1+(2/7)\mu\cos\sigma][1-(5/7)\mu'\cos\varphi](R\omega_o/v_o)}. \quad (45)$$

2.6. μ–s case

Here, sliding exists between spheres 1 and 2 during the impact event while stick occurs in the sphere 2-horizontal surface contact. In agreement with prior considerations, Eqs. (16)–(19) apply so that angles δ_1 and ϑ_1 are again described by Eqs. (22) and (24), respectively.

In this case, the impulses F_{fx},F_{fy} can be expressed as

$$F_{fx} = \frac{(2/7)m_1(1+e)v_o\cos\psi[1+(5/2)\mu\cos\sigma]}{1+M}, \quad (46)$$

$$F_{fy} = \frac{(2/7)m_1\mu(1+e)v_o\cos\psi\sin\sigma}{1+M}, \quad (47)$$

where σ is given by Eq. (16). Using Eqs. (5)–(12), and (46), (47), one obtains

$$\tan\delta_2 = \frac{\mu\sin\sigma}{1-\mu\cos\sigma}. \quad (48)$$

These equations, combined with Eqs. (14), (15) yield

$$\tan\vartheta_2 = \frac{(7/2+\mu')\mu\sin\sigma}{(7/2)(1-\mu\cos\sigma) + \mu'(1+(5/2)\mu\cos\sigma)}. \quad (49)$$

2.7. Impact regimes

As discussed in the preceding sections, four cases can be discerned within the approach presented here for two-sphere billiard-type collisions. Their occurrence depends significantly on the impact angle, ψ, the coefficients of restitution and friction, and the initial spin conditions, expressed in the foregoing set of equations by the $R\omega_o/v_o$ and $R\omega_{zo}/v_o\cos\psi$ ratios.

First of all, in the most single case where $R\omega_o/v_o = 1$; and $R\omega_{zo} = 0$; i.e., when the cue sphere is initially in pure rolling motion without additional 'English' spin, the transition from the stick regime to the sliding regime in the sphere 1–sphere 2 interaction occurs at a limiting impact angle, ψ_{LIM}, given by

$$\cos\psi_{LIM} = \frac{2}{7\mu_o(1+e)}, \quad (50)$$

where μ_o represents the static coefficient of friction in the contact between spheres 1 and 2, as described by Kane and Levinson [4]. For simplicity, in the following we consider $\mu_o = \mu$ in all cases, an approximation taken usually in both smooth and non-smooth theoretical approaches [3,7,10–13]. Remarkably, the transition angle is independent on the mass ratio, M, a situation described by Stronge [10].

The transition from slip–stick to gross slip can be graphically illustrated in terms of the dependency of F_{th} on the angle of impact, depicted in Fig. 4 for $e = 0.80$, using

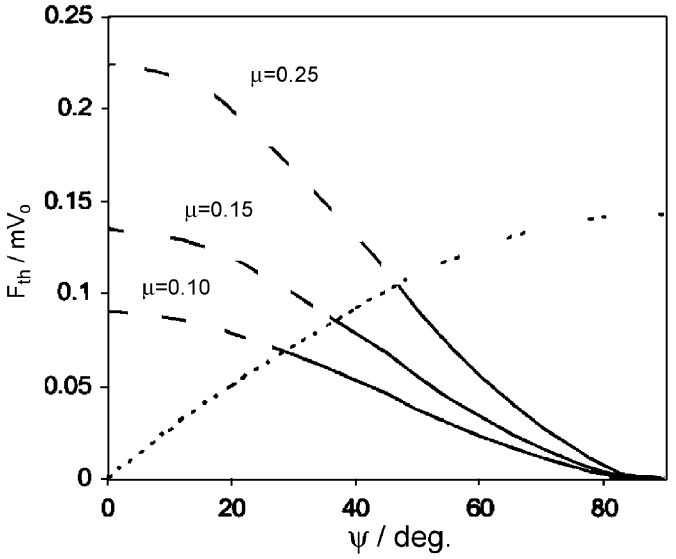

Fig. 4. Variation of F_{th} on ψ for the impact of spheres with $e = 1$. Dotted line: slip–stick case (Eq. (28)); continuous lines: gross slip case (Eq. (18)) with $\mu = 0.10$, 0.15, and 0.25.

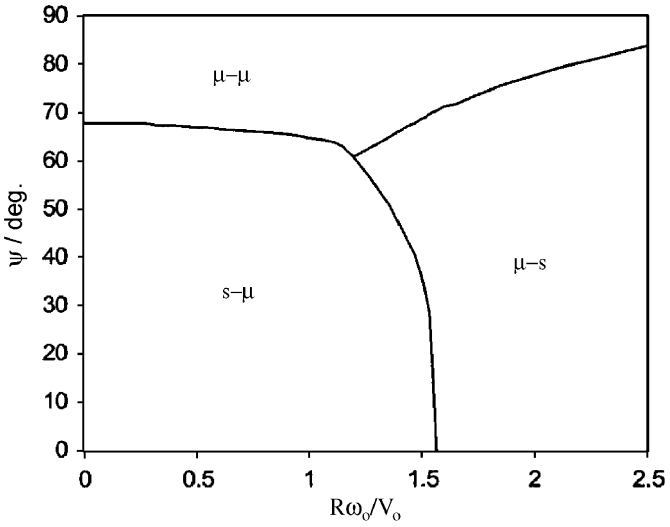

Fig. 5. Impact regimes in the impact angle/horizontal spin diagram for the collisions between rough spheres having $e = 0.50$, $\mu = 0.30$, $\mu' = 0.50$.

Eqs. (18) and (28). As we increase ψ, we move up the dotted line (stick regime) until we reach the solid line appropriate for the value of μ, so that on increasing the value of the coefficient of friction, the transition from stick to sliding occurs at larger angles of impact.

When sliding exists in the sphere 1–sphere 2 interaction, the transition from slip–stick to gross slip in the sphere 2-horizontal surface interaction takes place for

$$\mu^2\left(\frac{21}{4}-\frac{4}{49}\mu'^2\right)\cos^2\psi_{LIM}+5\mu\cos\psi_{LIM}+1+\mu^2=0. \tag{51}$$

As in the case of the sphere 1–sphere 2 interactions, the occurrence of stick or slip in the sphere 2-supporting surface interaction will depend on the tangential velocity/normal velocity, V_{2h}/V_{2v}, of the contacting point in the beginning of the contact. This ratio can be expressed as

$$\frac{V_{2h}}{V_{2v}}=\frac{\sqrt{(F_n+(5/2)F_{tv})^2+F_{th}^2}}{F_{tv}}. \tag{52}$$

Since in general F_n is clearly larger than F_{tv} and F_{th}, one can expect that the V_{2h}/V_{2v} ratio will be usually larger, so that sliding must prevail in the percussive contact between the sphere 2 and the supporting surface. In agreement with this, when stick exists in the sphere 1–sphere 2 interaction, the transition from slip–stick to gross slip in the sphere 2-horizontal surface interaction takes place for

$$\tan\psi_{LIM}=\sqrt{(49/4)\mu'^2-[(7/2)(1+e)+5/2]^2}. \tag{53}$$

These results indicate that the *s–s* regime can only be achieved for very high values of the coefficient of friction between the sphere 2 and the supporting surface.

Fig. 5 shows a two-dimensions diagram for collisions between identical rough spheres with $e = 0.50$; $\mu = 0.30$; $\mu' = 0.50$, taking the $R\omega_o/v_o$ ratio as an independent variable. For these parameter values, the *s–s* regime is entirely absent. For small values of $R\omega_o/v_o$ sliding prevails at high impact angles, thus defining the $\mu-\mu$ zone of the diagram. At low $R\omega_o/v_o$ and low impact angle values the *s–μ* regime is attained, while at low impact angles but large $R\omega_o/v_o$ values, the *μ–s* regime takes place. Roughly, the proposed formulation indicates that the occurrence of the *s–s* regime requires conjunction of relatively low friction in the sphere–sphere contact and high friction in the sphere–pool contact. Accordingly, for these parameter values, implying relatively high friction for sphere–sphere and sphere–pool contacts, the *s–s* regime is absent.

3. Experimental

Experiments on collisions between steel spheres (diameter 2.50 cm, mass 70.0 g) billiard ball and rubber ball (mass 46.4 g, diameter 4.60 cm) moving on a regulation billiard pool were performed. The velocity of the cue ball was adjusted to 0.75 ± 0.05 m/s using an auxiliary slanted track. The distance from the edge of the slanted track to the object ball was of 50 cm; this distance was great enough to ensure that the cue ball acquires pure rolling motion before the impact. Complementary experiments with billiard and rubber balls were made by projecting the cue ball with different initial spins with the help of a tapering rod. This was horizontally launched striking the surface of the cue ball in a point horizontally separated ca. 1 cm of the centre of the ball. The angles of impact, post-collision and post-transition were determined from the photographs recorded with a conventional camera placed in a vertical position 75 cm just over the point of contact between the

balls at the impact as previously described, using exposure times between 1.2 and 2.0 s [24].

4. Results and discussion

4.1. Rebound experiments

The suitability of the proposed non-smooth description of the slip–stick regime was tested by using experimental data provided by Johnson [14] for an elastic rubber ball striking a heavy steel plate at a small speed. This case can easily be derived from the foregoing set of equations by inserting $M = 0$. In Fig. 6, such experimental data are compared with theoretical predictions from the conventional non-smooth model (a) [6,7], the continuous models of Stronge (b) [10], and Maw et al. (c) [8,9], as well as the binary models from Walton and Foerster et al. (d) [27,28] and the current model (e). In this figure, the (tangential velocity of the point of contact at the end of the rebound)/(tangential velocity of this point at the beginning of the impact) ratio is plotted against the (tangential velocity of the point of contact at the beginning of the impact)/(normal velocity of this point at the beginning of the impact) one. Such $V_x/\mu V_{oy}$ vs. $V_{ox}/\mu V_{oy}$ plots defines two regions in the diagram corresponding to the slip–stick regime (left) and the common predictions for the gross slip regime (right).

Experimental data are far from the conventional discontinuous model represented by line (a) while are close to continuous models of Maw et al. (c) and Stronge (b). Binary models represented by line (d) also diverge clearly from experimental data. Interestingly, predictions derived from the current discontinuous approach (e) provide the better fit with experimental data in the slip–stick region of the diagram.

In Fig. 7, experimental data for the rebound of a rubber ball on a rough surface taken from Garwin [17] are compared with theoretical predictions for the slip–stick regime (continuous lines) with $\mu = 0.55$, and the sliding regime taking $e = 0.92$, and $\mu = 0.55$, 0.30, and 0.20 (discontinuous lines). In the region where gross slip occurs, a satisfactory agreement between experimental data and theory, using Eqs. (3) and (16)–(21) with $M = 0$, can be observed. As can be seen in Fig. 7, no conclusive data were available for the slip–stick region.

4.2. Two-sphere collisions

Two-sphere collision experiments involving rolling without spin prior to impact were performed with steel bearings, billiard ball and rubber balls. Experimental data provided a satisfactory agreement with predictions from the previously described models, the best fit between theory and experiment being obtained for the values of the coefficients of restitution and friction listed in Table 1. Fig. 8 shows a typical photograph recorded on a billiard pool, providing an image comparable with the scheme depicted in Fig. 1. Fig. 9 compares experimental data values of $\tan\delta_1$ (a) and $\tan\vartheta_1$ (b) vs. $\tan\psi$ with theoretical predictions for the oblique impact of rubber superballs.

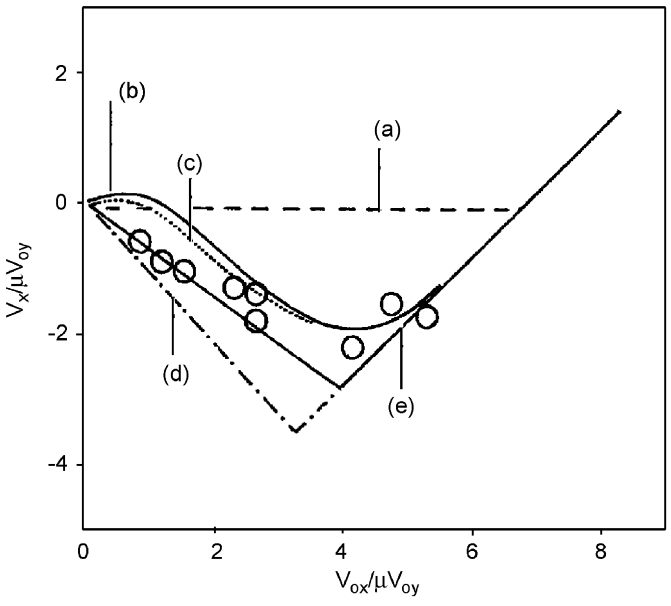

Fig. 6. Variation of tangential velocity of the contact point on elastic rubber superball striking a steel plate at instant of separation on the angle of incidence. Experimental data taken from Johnson [14]. Theoretical predictions from the Brach [3] and Kane and Levinson [4] formulations (a, - - -), Stronge [10–13] (b; —), Maw et al. [8,9] (c, …), Walton [26] and Foerster et al. [27] (d, .-.-), and the current model (e, —).

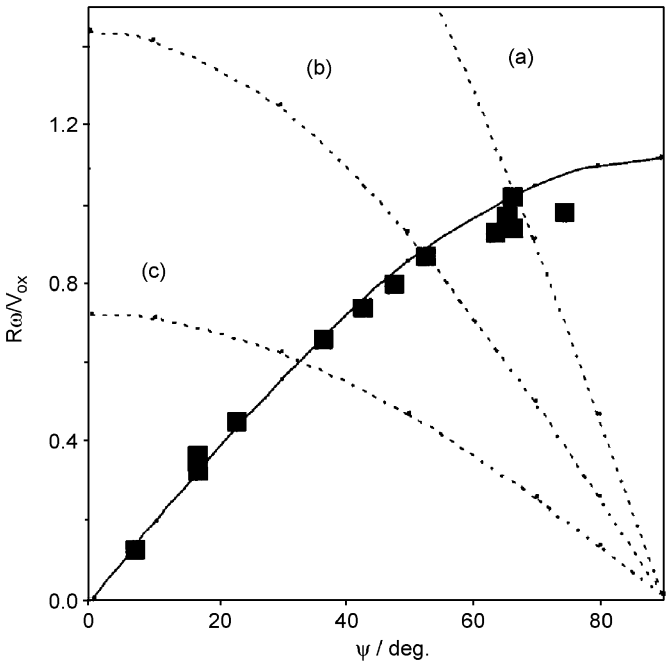

Fig. 7. Comparison of experimental data for the rebound of a rubber ball on a rough surface taken from Garwin [17] and theoretical predictions for the slip–stick regime (continuous line) with $\mu = 0.55$, and the gross slip regime taking $e = 0.92$, and $\mu = 0.55$ (a), $\mu = 0.30$ (b), and $\mu = 0.20$ (c). Gross line represents the 'best' fit of data defining a transition from stick–slip to gross slip.

Table 1
Values for the coefficients of restitution and friction for the studied materials determined from the best fit between theoretical equations (23), (24), (40) and (41) and experimental data

	Billiard balls	Steel bearings	Rubber balls	Billiard balls (Ref. [23])
Ball–ball coefficient of restitution	0.97 ± 0.02	0.92 ± 0.02	0.88 ± 0.03	0.93 ± 0.03
Ball–ball coefficient of friction (dynamic)	0.07 ± 0.02	0.14 ± 0.02	0.60 ± 0.03	0.06 ± 0.04
Ball–ball coefficient of friction (static)		0.18 ± 0.03		
Ball–table coefficient of friction (dynamic)	0.15 ± 0.02	0.15 ± 0.02	0.55 ± 0.03	0.10 ± 0.05

Comparison from the values recently provided by Alciatore [23].

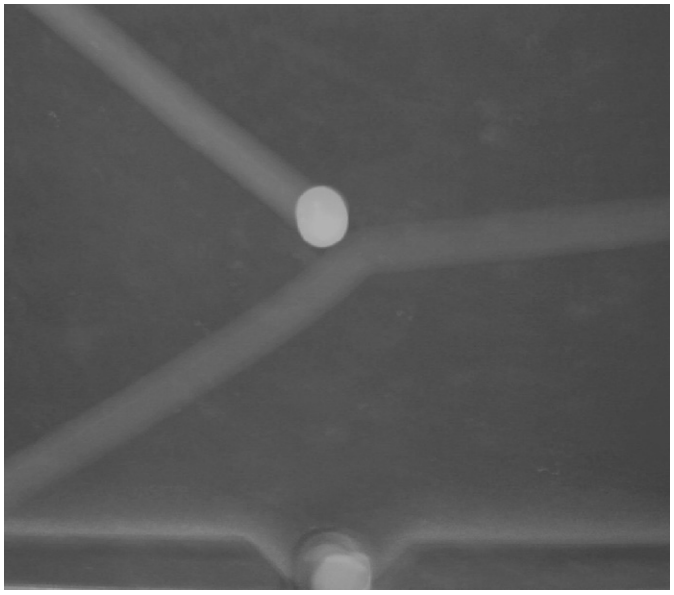

Fig. 8. Photograph taken at an exposure time of 2.0 s on a billiard-ball collision.

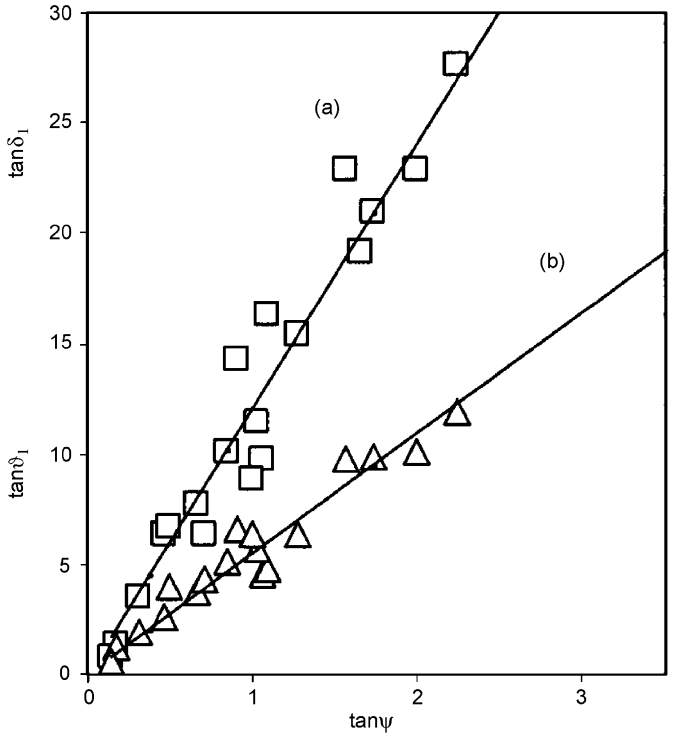

Fig. 9. Variation of values of $\tan\delta_1$ (squares, a) and $\tan\theta_1$ (triangles, b) on $\tan\psi$ for collisions of 'superball' rubber spheres. Theoretical lines for a slip–stick regime taking the values for e and μ in Table 1.

Here, the best fit of experimental data to theory was found for the s–μ model, inserting the values for e and μ presented in Table 1 into Eqs. (35) and (40). The predicted values for the angles δ_1 and ϑ_1, however, were close to those derived from the $\mu-\mu$ model using the above parameter values, so that experimental data using angles δ_1 and ϑ_1 were non-conclusive with regard to the transition from the s–μ regime to the $\mu-\mu$ one. Additionally, this transition should occur at a large angle of impact. As discussed below, transition from one impact regime to another is better monitored using the angle δ_2, for which largely separate predictions are obtained (*vide infra*).

For collisions between steel bearings experimental values of δ_1 and ϑ_1 angles agreed with theory from Eqs. (22) and (24) by taking the corresponding values (see Table 1) for e, μ and μ'. This can be seen in Fig. 10, where the experimental angles $\alpha_1(=\delta_1-\psi)$ and θ_1 are represented as a function of the angle of impact, ψ, for collisions between steel bearings. Continuous lines in this figure correspond to theoretical values for the sliding regime (Eqs. (22) and (24), whereas dotted lines correspond to the predictions from the s–μ regime (Eqs. (36) and (40)). In this case, the transition of stick–slip to gross slip takes place at a small angle of impact, so that only the $\mu-\mu$ regime was observed in practice.

For billiard-ball collisions, experimental data agree with theory from the $\mu-\mu$ model taking the values for e, μ and μ' summarized in Table 1. These values are similar to those reported by Marlow [22] recently revised by Alciatore [23]. Consistently with prior results [24], for these parameter values, only the gross slip regime is operative for collisions with $R\omega_o/v_o = 1$, $R\omega_{zo}/v_o = 0$; i.e., under these conditions, the slip–stick regime does not occur.

Variation of δ_2 with the impact angle illustrates the significant differences between the predictions of the gross slip and slip–stick regimes. As shown in Fig. 11, experimental data for billiard-ball collisions is close to theory for the $\mu-\mu$ regime (Eq. (23)), (continuous line (a)). This prediction is close to that from the μ–s model (Eq. (48), using the values for e, μ, and μ' (continuous line (b)) in Table 1. Experimental data, however, clearly diverges from

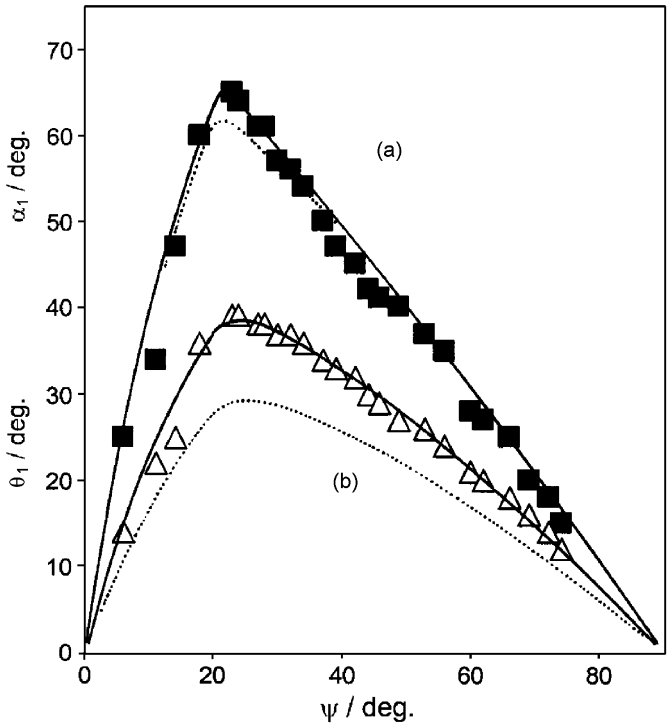

Fig. 10. Plots of $\alpha_1(=\delta_1-\psi)$ (a) and θ_1 (b) vs. the impact angle, ψ, for collisions between steel bearings ($M=1$). Continuous lines correspond to theoretical values for the $\mu-\mu$ regime (Eqs. (22) and (24)) inserting the values for e and μ summarized in Table 1. Dotted lines correspond to the predictions s–μ regime using these parameter values.

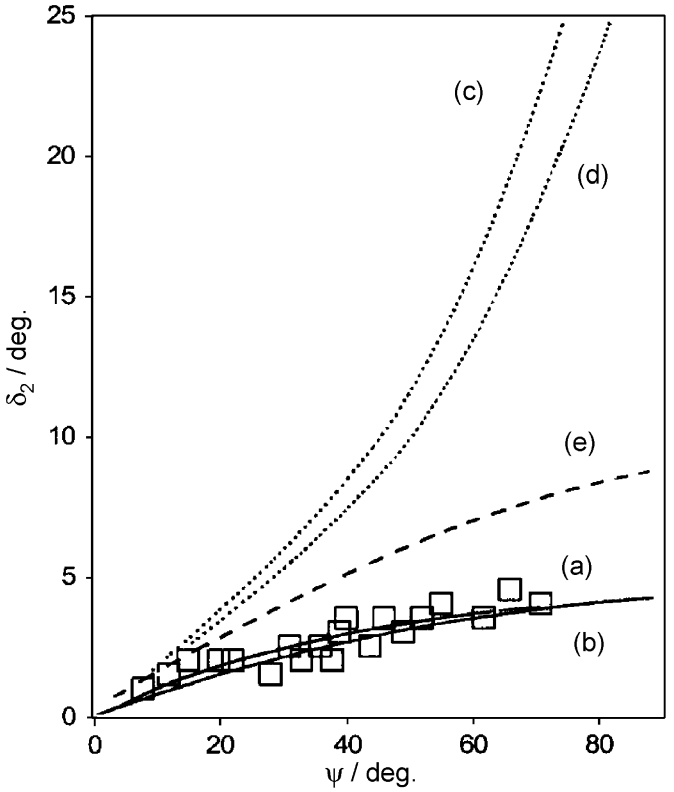

Fig. 11. Variation of δ_2 with the impact angle for billiard-ball collisions. Continuous lines: theory for $\mu-\mu$ (a) and μ–s (b) models; dotted lines: theory for s–s (c) and s–μ (d) models, all taking the values for e, μ, and μ' contained in Table 1, whereas dashed line (e) corresponds to theory for the $\mu-\mu$ model using $\mu=0.15$.

the predictions of the s–s (dotted line (c)) and s–μ (dotted line (d)) models, Eqs. (39) and (44), respectively, taking these parameter values. Interestingly, the gross slip model is sensitive to changes in the values of the coefficients of restitution and friction. This can also be seen on comparing experimental data in Fig. 11 with theory for the $\mu-\mu$ regime (dashed line (e)), taking $\mu=0.15$.

The transition from gross slip to slip–stick regimes can be studied in more detail using data for collisions between steel bearings depicted in Fig. 12, in which plots of δ_2 vs. ψ are shown. Here, experimental data at impact angles lower than 35° fit with Eq. (39), corresponding to the s–μ model, by taking the e and μ values in Table 1. At impact angles above 35°, the $\mu-\mu$ regime is attained and experimental data fit with Eq. (23) using those values for e and μ.

As shown in Fig. 12, experimental data appear to define a 'jump' in the δ_2 vs. ψ curve. This feature can be rationalized on considering that the transition from the gross slip to slip–stick regime must occur at a limiting impact angle, ψ_L, at which the friction force reaches its limiting value given by the value of the static coefficient of friction, μ_o, as formulated in Eq. (50). Since in general $\mu_o\neq\mu$, a discontinuity in the δ_2 vs. ψ plots may appear in the transition from one regime to another. Experimental data in Fig. 12 permits to estimate a value for the static coefficient of restitution of $\mu_o=0.18$, because the maximum δ_2 value in the 'jump' is located near the

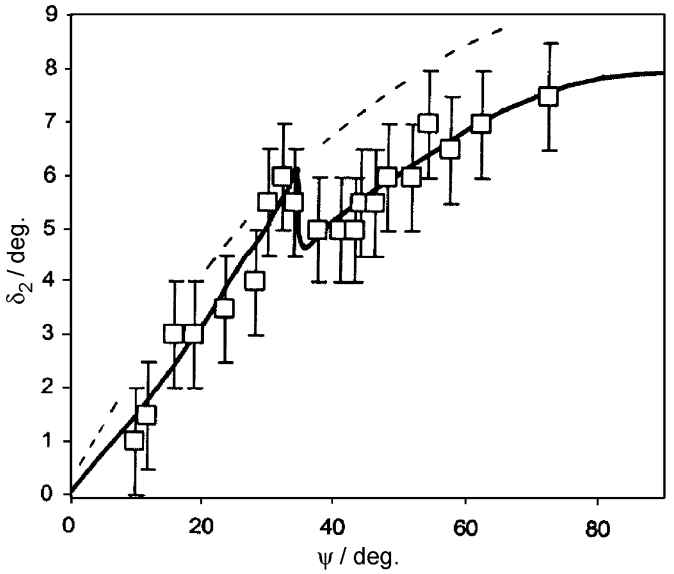

Fig. 12. Comparison of theoretical and experimental variation of δ_2 with ψ for collisions of steel bearings. Continuous line corresponds to theory for a transition from s–μ to $\mu-\mu$ regimes taking the values for e , μ and μ' presented in Table 1 and taking a 'jump' corresponding to a static coefficient of friction of $\mu_o=0.18$. Dotted line corresponds to theoretical gross slip regime using the above values for e, μ and μ' in Table 1.

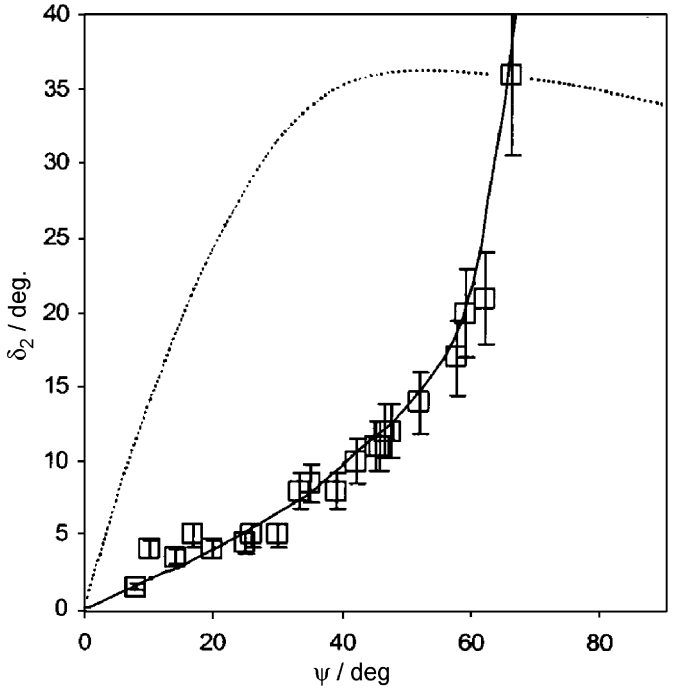

Fig. 13. Plots of δ_2 vs. impact angle for the impact of rubber spheres and theoretical expectances for the s–μ (continuous line) and $\mu-\mu$ (dotted line) models taking the values for e and μ shown in Table 1.

corresponding theoretical gross slip curve (dotted line in Fig. 12).

Plots of δ_2 vs. ψ for the impact of rubber balls provided a remarkably different behaviour. As shown in Fig. 13, the impact of rubber spheres is dominated by the slip–stick regime, experimental data fitting with theoretical values obtained by substituting the e and μ values presented in Table 1 into Eq. (39) (s–μ model, continuous line). Here, the $\mu-\mu$ (dotted line) or μ–s regimes are attained only for a large impact angle (ca. 74°) using the above parameter values.

4.3. Billiards and superbilliards

Interestingly, the described approach can be used for predicting the paths of the spheres in billiards and pools for different spin effects. Thus, the approximate paths in billiard-ball ($M = 1$) collisions at an impact angle of 45° with no initial pivotment ($R\omega_{zo}/v_o = 0$) and arbitrary forward 'English' spin are depicted in Fig. 14. Here, Eqs. (22)–(25), corresponding to the $\mu-\mu$ model are taken, inserting the values for e , μ and μ' listed in Table 1. A similar representation is given in Fig. 15 for collisions between rubber balls ('superbilliard' collisions) under similar conditions. Here, the s–μ model (Eqs. (39)–(41)), was taken to be operative using the above values for e and μ.

The obtained representations indicate that, for billiard-ball collisions, the path of the cue ball after the impact is strongly influenced by the value of the $R\omega_o/v_o$ ratio, while the trajectory of the object ball remains almost insensitive

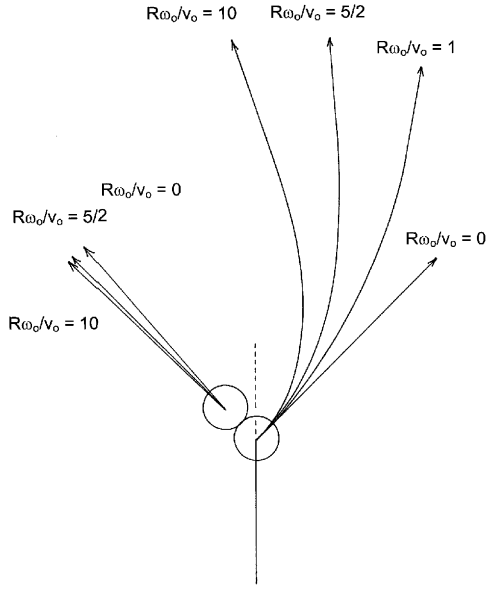

Fig. 14. Theoretical (approximate) paths for selected $R\omega_o/v_o$ values for the impact between regulation billiard balls at $\psi = 45°$ from Eqs. (22)–(25), taking the $\mu-\mu$ model with $M = 1$, $R\Omega_o/v_o = 0$, $e = 0.97$, $\mu = 0.07$, $\mu' = 0.15$.

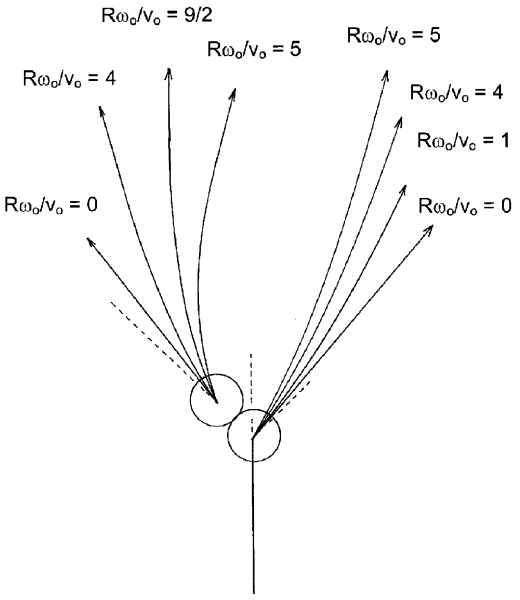

Fig. 15. Theoretical (approximate) paths for selected $R\omega_o/v_o$ values for the impact between rubber superballs balls at $\psi = 45°$ using Eqs. (35)–(41), taking the s–μ model with $M = 1$, $R\Omega_o/v_o = 0$, $e = 0.88$.

to changes in the 'English' spin. On the contrary, for rubber balls, the path of the cue ball lightly varies with the $R\omega_o/v_o$ ratio, whereas the path of the object ball experiences significant variations with that ratio. Similar results were obtained for the variations of the paths with the initial spin about a vertical axis (spin of pivotment, $R\omega_{zo}/v_o$) when the cue ball is initially moving in pure rolling motion ($R\omega_o/v_o = 1$).

These paths differ remarkably from those predicted from the frictionless model of Wallace and Schroeder [2]. In this

model there is no account for impulsive frictional forces, so that no dependence of post-collision paths on the initial 'English' spins can be predicted. A series of additional experiments was performed by horizontally striking the cue ball with a tapering rod at a point separated ca. 1 cm at the left or at the right from the ball centre. Here, the cue ball was projected with a given pivotment spin. Although a control of the initial pivotment spin of the cue ball was unavailable, the trajectories of the balls were close to those theoretically expected for pivotment spins ($R\omega_{zo}/v_o$) between $+0.3$ and -0.3.

5. Conclusions

The impact of a cue ball moving with arbitrary 'English' spins along a rough horizontal surface against a stationary object ball can be described in terms of a single discontinuous model incorporating effects of inelasticity and friction in the percussive ball–ball and ball-supporting surface events. As a result, a series of velocity-independent equations relating the post-collision and post-transition angles of scattering after the impact with the impact angle, the mass ratio and the coefficients of restitution and friction is obtained. This includes provisions for different regimes of impact, including gross slip and slip–stick regimes close to those predicted by smooth models. The scope of this formulation is obviously conditioned by the validity of the simplifying assumptions concerning the constancy of the coefficients of restitution and friction and the discontinuous representation of the impact event.

In spite of these limitations, the current discontinuous approach to two-sphere collisions in billiard-type experiments provides predictions in close agreement with available experimental data, thus suggesting that there is place for a judicious use of that approximation in the context of a discontinuous formulation of the impact.

References

[1] Coriolis G. Théorie mathématique des effects du jeu de billard. Paris: Carilian-Goeury Librairie; 1835.

[2] Wallace RE, Schroeder MC. Analysis of billiard ball collisions in two dimensions. American Journal of Physics 1988;56:815–9.

[3] Brach RM. Friction, restitution, and energy loss in planar collisions. ASME Journal of Applied Mechanics 1984;51:164–70.

[4] Kane TR, Levinson DA. An explicit solution of the general two-body collision problem. Computational Mechanics 1987;2:75–87.

[5] Smith CE. Predicting rebounds using rigid-body dynamics. ASME Journal of Applied Mechanics 1991;58:754–8.

[6] Chatterjee A, Ruina A. New algebraic rigid-body collision law based on impulse space considerations. ASME Journal of Applied Mechanics 1998;65:939–51.

[7] Keller JB. Impact with friction. ASME Journal of Applied Mechanics 1986;53:1–4.

[8] Maw N, Barber JR, Fawcett JN. The oblique impact of elastic spheres. Wear 1976;38:101–14.

[9] Maw N, Barber JR, Fawcett JN. The role of elastic tangential compliance in oblique impact. Journal of Lubrication Technology 1981;103:74–80.

[10] Stronge WJ. Rigid body collisions with friction. Proceedings of the Royal Society London 1990;A431:169–81.

[11] Stronge WJ. Two-dimensional rigid-body impact with friction-discussion. ASME Journal of Applied Mechanics 1993;60:564–6.

[12] Stronge WJ. Planar impact of rough compliant bodies. International Journal of Impact Engineering 1994;15:435–50.

[13] Stronge WJ, James R, Ravani B. Oblique impact with friction and tangential compliance. Philosophical Transactions of the Royal Society London 2001;A359:2447–65.

[14] Johnson KL. The bounce of 'superball'. International Journal of Mechanical Engineering Education 1983;111:57–63.

[15] Ko PL. The significance of shear and normal force components of tube wear due to fretting and periodic impacting. Wear 1985;106: 261–81.

[16] Lewis AD, Rogers RJ. Experimental and numerical study of forces during oblique impact. Journal of Sound Vibration 1988;125: 403–12.

[17] Garwin R. Kinematics of ultraelastic rough ball. American Journal of Physics 1969;37:88–92.

[18] Cross R. Grip-slip behaviour of a bouncing ball. American Journal of Physics 2002;70:1093–102.

[19] Walker J. The physics of the follow, the draw and the massé (in billiards and pools). Scientific American 1983;249:127–9.

[20] Kondic L. Dynamics of spherical particles on a surface: collision-induced sliding and other effects. Physical Review E 1999;60:751–70.

[21] Dutt M, Behringer RP. Effects of surface friction on a two-dimensional granular system: cooling bound system. Physical Review E 2004;70:061304–15.

[22] Marlow WC. Physics of pocket billiards. American Institute of Physics; 1994.

[23] Alciatore DG. The illustrated principles of pool and billiards. New York: Sterling Publishers; 2004.

[24] Doménech A, Doménech MT. Oblique impact of rolling spheres: a generalization of billiard-ball collisions. Revista Mexicana de Física 1998;44:611–8.

[25] Doménech A. A classical experiment revisited: the bounce of balls and superballs in three dimensions. American Journal of Physics 2005;73:28–36.

[26] Hopkins DC, Patterson JD. Bowling frames: paths of a bowling ball. American Journal of Physics 1977;45:263–6.

[27] Walton OR. Numerical simulation of inelastic, frictional particle–particle interactions. In: Roco MC, editor. Particluate two-phase flow. New York: Butterworth-Heineman; 1992. p. 884–911.

[28] Foerster SF, Longe MY, Chang H, Allia K. Measurement of collision properties of small spheres. Physics of Fluids 1994;6:1108–13.

[29] Hutchings IM, Macmillan NH, Rickerby DG. Further studies of the oblique impact of hard sphere against a ductile solid. International Journal of Mechanical Sciences 1981;23:639–41.

[30] Although this situation may be operative in several instances, such as in the impact of a tennis ball with a rough surface, representation in Fig. 3 obviously overestimates the size of the deformed region in the case of billiard balls, and must be taken merely as a rough view of the impact event.